



A HUBBLE SPACE TELESCOPE STUDY OF THE ENIGMATIC MILKY WAY HALO GLOBULAR CLUSTER CRATER*

DANIEL R. WEISZ^{1,9}, SERGEY E. KOPOSOV², ANDREW E. DOLPHIN³, VASILY BELOKUROV², MARK GIELES⁴, MARIO L. MATEO⁵,
EDWARD W. OLSZEWSKI⁶, ALISON SILLS⁷, AND MATTHEW G. WALKER⁸

¹ Astronomy Department, Box 351580, University of Washington, Seattle, WA, USA; dweisz@uw.edu

² Institute of Astronomy, University of Cambridge, Madingley Road, Cambridge, CB3 0HA, UK

³ Raytheon Company, Tucson, AZ, 85734, USA

⁴ Department of Physics, University of Surrey, Guildford GU2 7XH, UK

⁵ Department of Astronomy, University of Michigan, 311 West Hall, 1085 S. University Avenue, Ann Arbor, MI 48109, USA

⁶ Steward Observatory, The University of Arizona, 933 N. Cherry Avenue., Tucson, AZ 85721, USA

⁷ Department of Physics and Astronomy, McMaster University, Hamilton, ON L8S 4M1, Canada

⁸ McWilliams Center for Cosmology, Department of Physics, Carnegie Mellon University, 5000 Forbes Avenue, Pittsburgh, PA 15213, USA

Received 2015 November 3; accepted 2016 February 25; published 2016 May 2

ABSTRACT

We analyze the resolved stellar populations of the faint stellar system, Crater, based on deep optical imaging taken with the Advanced Camera for Surveys on the *Hubble Space Telescope*. Crater’s color–magnitude diagram (CMD) extends ~ 4 mag below the oldest main-sequence (MS) turnoff. Structurally, we find that Crater has a half-light radius of ~ 20 pc and no evidence for tidal distortions. We model Crater’s CMD as a simple stellar population (SSP) and alternatively by solving for its full star formation history. In both cases, Crater is well described by an SSP with an age of ~ 7.5 Gyr, a metallicity of $[M/H] \sim -1.65$, a total stellar mass of $M_* \sim 1e4 M_\odot$, and a luminosity of $M_V \sim -5.3$, located at a distance of $d \sim 145$ kpc, with modest uncertainties due to differences in the underlying stellar evolution models. We argue that the sparse sampling of stars above the turnoff and subgiant branch are likely to be $1.0\text{--}1.4 M_\odot$ blue stragglers and their evolved descendants, as opposed to intermediate-age MS stars. We find that Crater is an unusually young cluster given its location in the Galaxy’s outer halo. We discuss scenarios for Crater’s origin, including the possibility of being stripped from the SMC or the accretion from lower-mass dwarfs such as Leo I or Carina. Despite uncertainty over its progenitor system, Crater appears to have been incorporated into the Galaxy more recently than $z \sim 1$ (8 Gyr ago), providing an important new constraint on the accretion history of the Galaxy.

Key words: Galaxy: halo – globular clusters: general – Hertzsprung–Russell and C–M diagrams

1. INTRODUCTION

The Sloan Digital Sky Survey (SDSS; York et al. 2000) has revolutionized our understanding of the faintest stellar systems. The deep, wide-field imaging of SDSS facilitated the discovery and characterization of dozens of faint dwarf galaxies and globular clusters (GCs) in and around the Milky Way (MW; e.g., Willman et al. 2005a, 2005b; Belokurov et al. 2006, 2007, 2009, 2010; Zucker et al. 2006a, 2006b; Irwin et al. 2007; Koposov et al. 2007; Kim et al. 2015a) and has proven transformative for our understanding of the nature of dark matter, the impact of cosmic reionization in the local universe, and how stars form in extremely shallow gravitational potentials (e.g., Simon & Geha 2007; Bovill & Ricotti 2009; Brown et al. 2014; Weisz et al. 2014a).

The faint object renaissance catalyzed by SDSS has continued to grow as new wide-field photometric surveys scan previously underexplored regions of the sky. Within the past year, dozens of new faint objects have been discovered in the south (e.g., Koposov et al. 2015a; Laevens et al. 2015a, 2015b; Martin et al. 2015; The DES Collaboration et al. 2015a, 2015b), dramatically increasing the census of known faint stellar systems, including the putative satellite

galaxies of the LMC (e.g., Koposov et al. 2015b; Simon et al. 2015; Walker et al. 2015).

Among the first objects discovered in this new era was Crater¹⁰ (Belokurov et al. 2014; Laevens et al. 2014). Crater appears to be a predominantly ancient and metal-poor system, similar to the majority of MW GCs and many of the faintest MW satellites. However, the presence of stars near the “blue loop” and above the oldest subgiant branch (SGB) led Belokurov et al. (2014) to speculate that Crater may have had multiple generations of star formation, unlike the majority of stellar systems of similar size, luminosity, and proximity to the MW. The presence of multiple, recent epochs of star formation in Crater would provide qualitatively new insight into how such extremely low mass objects can retain or accrete fresh gas and form stars, despite having such shallow potentials and being well within the virial radius of the MW.

However, there has been considerable debate over whether Crater is a GC or a faint galaxy. The codiscovery paper by Laevens et al. (2014) concluded that Crater is a GC with an unusually large size ($r_h \sim 20$ pc) and distance ($d_\odot \sim 145$ kpc). Stellar spectroscopy by Kirby et al. (2015) demonstrated that three of the four luminous putative blue loop stars are actually low-mass MW foreground stars, effectively ruling out star formation in Crater within the past Gyr. This study also revealed a small spread in metallicity and a stellar velocity

* Based on observations made with the NASA/ESA *Hubble Space Telescope*, obtained at the Space Telescope Science Institute, which is operated by the Association of Universities for Research in Astronomy, Inc., under NASA contract NAS 5-26555. These observations are associated with program #13746.

⁹ Hubble Fellow.

¹⁰ Independent codiscovery resulted in multiple names for this object: Crater, Laevens I, PSO J174.0675-10.87774. We have adopted “Crater” for this paper.

dispersion that appears consistent with a system made entirely of baryons. They also conclude that Crater is a GC.

In contrast, Bonifacio et al. (2015) argue that Crater is more likely to be a dwarf galaxy. Based on spectroscopy of two red giant branch (RGB) stars, they find a velocity dispersion that is larger than expected if only baryons were present. Face-value interpretation of this result implies the existence of dark matter and thus categorizes Crater as a galaxy (Willman & Strader 2012), although Bonifacio et al. (2015) acknowledge that the small number of stars and uncertainties on their velocities make this a tentative conclusion. Moreover, Bonifacio et al. (2015) show that the sparse sampling of stars above the oldest SGB are consistent with a ~ 2 Gyr stellar isochrone, which is incompatible with Crater being a simple stellar population (SSP).

However, this region of the color–magnitude diagram (CMD) is also occupied by blue stragglers, the products of binary star evolution, and their descendants, which can mimic the presence of intermediate-age single stars (e.g., Ferraro et al. 2015). Unfortunately, the faintness of these sources makes follow-up spectroscopy prohibitively expensive at this time, and we must rely on other means for interpretation.

In this paper, we present deep optical imaging of Crater taken with the *Hubble Space Telescope* (*HST*) and characterize its stellar populations by analyzing the resulting deep CMD. The *HST*-based CMD extends several magnitudes fainter than existing ground-based data, providing a new perspective on the nature of Crater. Using CMD analysis methods that are routinely applied to Local Group and nearby dwarf galaxies (e.g., Weisz et al. 2011, 2014a), we undertake a detailed characterization of Crater’s stellar populations and conclude that it is a GC and not a dwarf galaxy.

This paper is organized as follows. In Sections 2 and 3, we present the observations, describe the data reduction, discuss the CMD, and derive the structural parameters of Crater. In Section 4, we summarize our method of CMD analysis, and we present the results in Section 5. Finally, in Section 6, we examine Crater in the context of known dwarf galaxies and the MW GC population and discuss possible formation and accretion scenarios.

2. OBSERVATIONS AND DATA REDUCTION

Observations of Crater were taken with Advanced Camera for Surveys (ACS; Ford et al. 1998) aboard *HST* on 2014 November 11 and 12 as part of HST-GO-13746 (PI: M. Walker). The observations consisted of deep integrations in F606W (*R* band) and F814W (*I* band) with multiple exposures to mitigate the impact of cosmic rays. We did not dither to fill the chip gap as Crater easily fit on one ACS chip. The basic properties of Crater and our observations are listed in Table 1, and a false-color image of Crater is shown in Figure 1.

We performed point-spread function photometry on each of the charge transfer efficiency corrected (f_lc) images using DOLPHOT, an updated version of HSTPHOT (Dolphin 2000) with *HST*-specific modules. The parameters used for our photometry follow the recommendations in Williams et al. (2014).

We culled the catalog of detected objects to include only well-measured stars by requiring $\text{SNR}_{\text{F606W}} > 5$, $\text{SNR}_{\text{F814W}} > 5$, $(\text{sharp}_{\text{F606W}} + \text{sharp}_{\text{F814W}})^2 < 0.1$, and $(\text{crowd}_{\text{F606W}} + \text{crowd}_{\text{F814W}}) < 1.0$. Definitions of each of these parameters can be found in Dolphin (2000). We characterized completeness and photometric uncertainties using

Table 1
Observational and Structural Properties of Crater

Quantity	Value
R.A. (J2000)	11:36:16.5
Decl. (J2000)	−10:52:37.1
Obs. dates	2014 Nov 11 and 12
Exp. time (F606W, F814W) (s)	3915, 4095
50% completeness (F606W, F814W)	27.6, 27.1
Stars in CMD	3620
Distance (kpc)	145 ± 3
M_V	-5.3 ± 0.1
M_* ($10^3 M_\odot$)	$9.9^{+0.1}_{-0.05}$
$r_{1/2,\text{Plummer}}$ (arcsec)	0.46 ± 0.01
$r_{1/2,\text{Plummer}}$ (pc)	19.4 ± 0.4
$r_{1/2,\text{exponential}}$ (arcsec)	0.43 ± 0.01
$r_{0,\text{King}}$ radius (arcsec)	0.39 ± 0.02
$c = \log(r_i/r_0)$	0.76 ± 0.05
$1 - b/a$	< 0.055 (90%)

Note. Observational and structural properties of Crater. The distance, stellar mass, absolute luminosity, and structural parameters were computed from our analysis of Crater’s *HST*-based CMD.

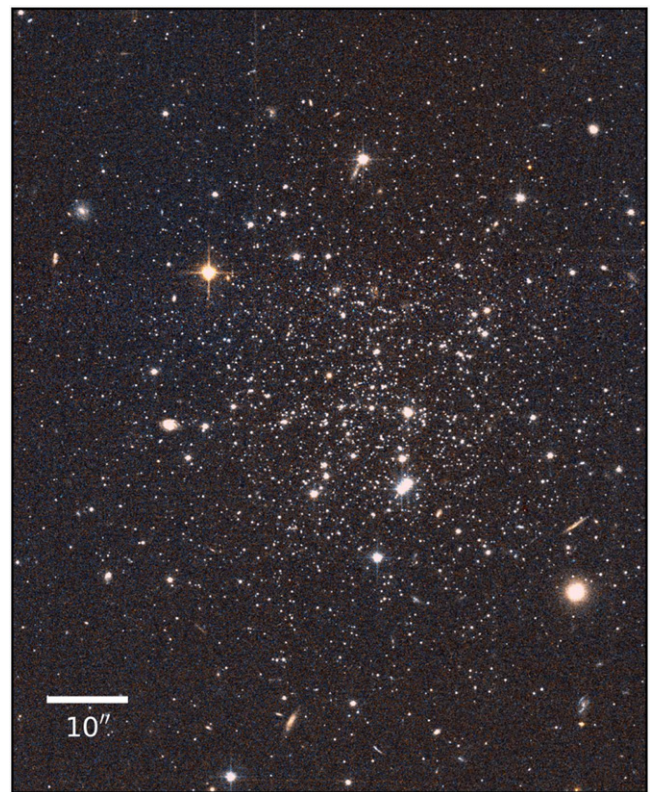


Figure 1. Colorized cutout of the composite F606W and F814W *HST*/ACS image of Crater.

$\sim 50,000$ artificial star tests (ASTs). We plot the completeness fractions in Figure 2. The similarity of completeness fractions as a function of radius confirms that our observations of Crater are not particularly crowded, even in the central regions. Our *HST* photometric catalog is available through MAST.¹¹

¹¹ <https://archive.stsci.edu/hst/>

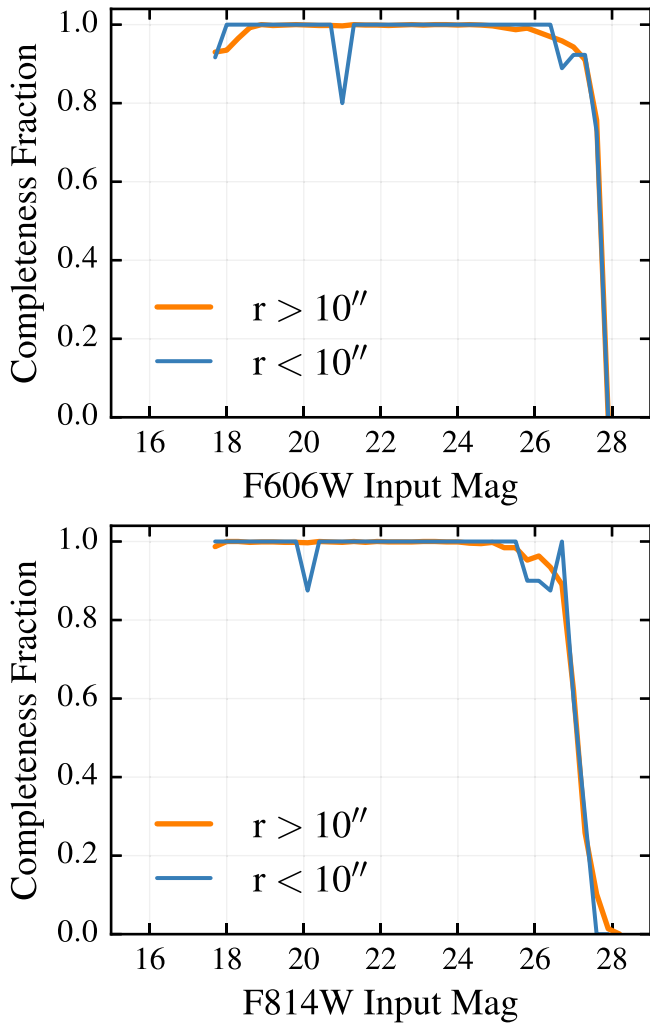


Figure 2. Completeness fractions vs. F606W and F814W input magnitude from our artificial star tests. We plot them for two differential radial regions to show that the completeness functions do not strongly vary with position. The jaggedness of the inner region profiles (blue) reflects the relatively small number of stars in a given magnitude bin.

3. THE DATA

3.1. The CMD and Membership Identification

We plot the *HST*/ACS CMD of Crater in Figure 3. Crater is clearly a predominantly older stellar system ($\gtrsim 3$ Gyr), based on the lack of a luminous main sequence (MS). In terms of population complexity, the narrowness of the RGB, oldest MS turnoff (MSTO), and extent of the main SGB suggests that the majority of stars in Crater were formed with a similar age and metallicity. The presence of a red clump and absence of a blue horizontal branch indicate that Crater is not an ancient and extremely metal-poor system, such as M92 or MW satellites of similar luminosity (e.g., VandenBerg et al. 2013; Brown et al. 2014). As noted in Belokurov et al. (2014), Crater’s horizontal branch appears to be unusually red for its metallicity, when compared to other MW GCs.

Beyond these dominant attributes, the CMD of Crater exhibits several secondary features. The first is a set of four luminous stars located at $F606W \sim 19$ and $F606W - F814W \sim 0.5$ identified by Belokurov et al. (2014) as putative blue loop stars with ages < 1 Gyr. If these are

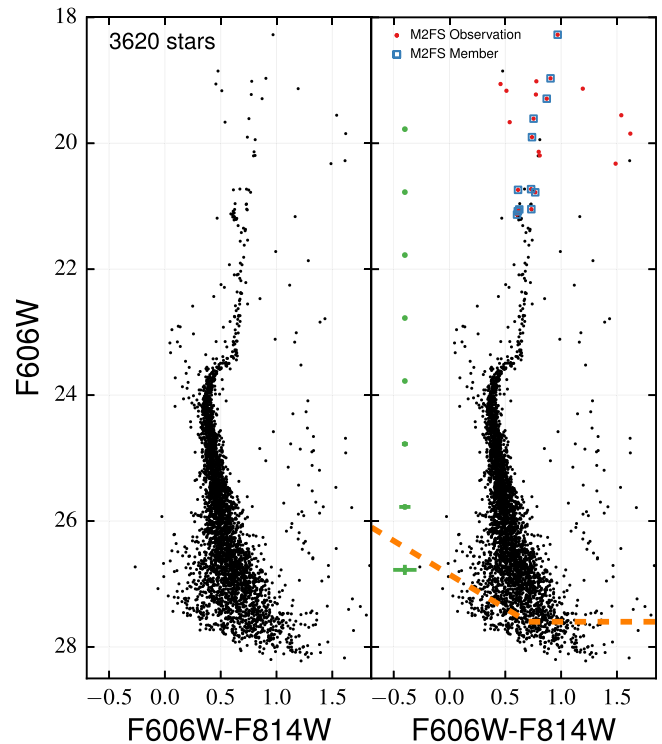


Figure 3. *HST*/ACS CMD of Crater. The red points in the right panel indicate stars with *Magellan*/M2FS spectroscopy. Those in blue squares are confirmed members of Crater. The photometric uncertainties are shown in green, and the 50% completeness limit, as determined by ASTs, is indicated by the orange dashed line.

bona fide “blue loop” stars, we would expect to see a larger number of luminous blue stars corresponding to the young MS brighter than $F606W \sim 21$. None are observed.

A second interesting feature is located immediately above the primary SGB at $F606W \sim 23.5$ and $F606W - F814W \sim 0.2$. The colors and magnitudes of these stars are consistent with either being ~ 2 – 5 Gyr old MS stars or blue stragglers. From the bright end of this feature, another set of stars extends diagonally up to $F606W \sim 22$, where it intersects with the RGB. Bonifacio et al. (2015) identify these stars as being consistent with a ~ 2 Gyr MSTO and SGB with a photometric metallicity of $[M/H] = -1.5$.

Finally, the set of stars located to the red of the RGB at $F606W - F814W \sim 1.3$ – 1.5 at all magnitudes are likely low-mass MW foreground stars. Such stars are also likely to overlap with other parts of the CMD, notably the RGB, which can lead to confused interpretation of the stellar populations. However, the number and CMD distribution of putative foreground sources appear well matched to models of distribution of MW stars (e.g., Girardi et al. 2005; de Jong et al. 2010), allowing for straightforward accounting of intervening sources.

To aid in identification and removal of nonmembers, we use stellar spectroscopy obtained with the Michigan/*Magellan* Fiber System (M2FS; Mateo et al. 2012) on the *Magellan*/Clay telescope as described in M. Mateo (2016, in preparation). Stars observed with M2FS are indicated by red points in the right panel of Figure 3. Only those enclosed within blue squares are likely members. The M2FS spectroscopy shows that three of the four putative blue loop stars are not members of Crater. Instead, they are foreground stars, which is consistent with the spectroscopic findings presented in Kirby et al. (2015).

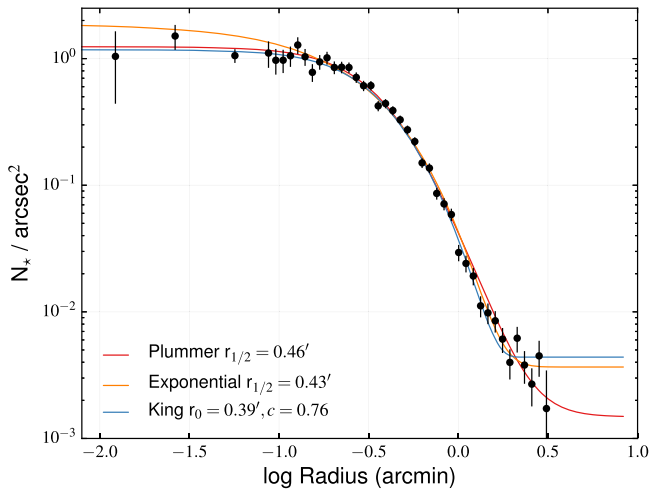


Figure 4. Radial stellar density profile of Crater based on our *HST* photometric catalog. The red, orange, and blue lines indicate the best-fit Plummer, exponential, and King profiles, respectively.

The Kirby et al. (2015) analysis of the fourth “blue loop” star has proven inconclusive. It has a systematic velocity that is close to that of Crater, which would favor it being a member. However, it would take an extremely unusual star formation history (SFH) or initial mass function (IMF) sampling to produce a single, young blue star.

The M2FS spectroscopically confirmed members trace out a narrow RGB and the red clump. Unfortunately, spectroscopy of stars fainter than the red clump is prohibitively expensive at this time.

3.2. Structural Parameters

We leverage the exquisite depth of the *HST* data to investigate the spatial structure of Crater. Specifically, we model the distribution of stars in Crater with two-dimensional elliptical Plummer, exponential, and spherical, single-component King (1966) models following the procedure described in Koposov et al. (2015a).

For the purposes of this analysis, we only use objects classified as stars with $F606W < 27$ to ensure high completeness ($>90\%$) across the entire catalog. We also remove obvious contamination from MW dwarf stars redward of the Crater MS and RGB ($F606W - F814W \gtrsim 1$).

The model parameters we use to describe Crater’s structure are as follows: Crater’s center, half-light radius, ellipticity, positional angle, surface density of background stars, and central surface density. For the King model we assume zero ellipticity and fit for the central dimensionless potential ϕ_0 , radius, and background density using the publicly available Python library *limipy* (Gieles & Zocchi 2015). For each model, we sample the posterior probability distribution with a Markov Chain Monte Carlo (MCMC) technique, assuming uniform priors on all parameters. The resulting measurements from marginalized distributions for the main parameters are listed in Table 1.

Aside from ellipticity, all of the marginalized distributions are well described by Gaussians. In Figure 4, we plot the one-dimensional density profile of Crater together with the most probable Plummer, exponential, and King models. The observed density profile shows no significant deviations from either model. The maximum likelihood value is somewhat

higher for the King fit than for the Plummer fit ($\Delta \log(L) \sim 4$) and the exponential fit ($\Delta \log(L) \sim 8$), but this is expected given the King model’s extra free parameter.

Additionally, we note that the best-fit concentration for the King model ($c = 0.76$) is low compared to other GCs. Only 20 out of 157 MW GC clusters have a lower concentration (e.g., Harris 1996). Most of these are “young halo” clusters, for which it has been pointed out that their concentration is lower (i.e., large core radii) than for old halo clusters and bulge/disk clusters. This structural property is also found for clusters in external dwarf galaxies (Mackey & Gilmore 2004).

From this modeling, we find that Crater has an ellipticity of <0.055 at 90% confidence level, indicating that it is consistent with being circular. The measured half-light radius from the Plummer fit is $r_{1/2} = 0.46 \pm 0.01$, which is consistent with the measurement of Laevens et al. (2014) and is 30% smaller than the estimate in Belokurov et al. (2014). The half-light radius measured using an exponential density profile is $r_{1/2} = 0.43 \pm 0.01$ and is consistent with the half-light radius implied by the King fit (0.42 ± 0.01). Assuming a heliocentric distance of 145 kpc, the half-light radius of Crater is 19.4 ± 0.4 pc. The combination of being circular and well described by a Plummer profile suggests that Crater is unlikely to have experienced drastic tidal stripping.

4. METHODOLOGY

We analyze the stellar populations of Crater using the CMD modeling software package *MATCH* (Dolphin 2002). In brief, *MATCH* requires a user-specified stellar evolution library, stellar IMF, binary fraction, and search ranges in distance, extinction, age, and metallicity. For a given combination of these parameters, *MATCH* constructs a set of SSPs that are linearly combined to form a composite CMD. The weight of each SSP is the star formation rate (or total stellar mass) at that age/metallicity combination. The composite CMD is then convolved with the observational noise model (photometric uncertainties and completeness) as determined by the ASTs. Finally, the synthetic and observed CMDs are compared in bins of color and magnitude of specified size (0.05 and 0.1 mag, respectively), and the probability of the observed CMD given the synthetic CMD is computed using a Poisson likelihood function. More details on the general methodology of *MATCH* can be found in Dolphin (2002).

We model Crater’s CMD in two ways: first by assuming that it is an SSP, and second by solving for its full SFH. In both cases we used the parameters listed in Table 2 and employed two different stellar evolution libraries, Dartmouth (Dotter et al. 2008) and PARSEC (Bressan et al. 2012), in order to quantify the sensitivity of our result to the choice of stellar evolution model. While the PARSEC models are currently only available with solar-scaled abundances, i.e., $[\alpha/\text{Fe}] = 0.0$, the Dartmouth models allowed us to explore several α -enhancements ranging from $[\alpha/\text{Fe}] = -0.2$ to $+0.4$.

We took an iterative approach to modeling the CMD such that we started with coarse resolution searches in distance and extinction (0.05 dex resolution) and, upon convergence, used a finer grid resolution (0.01 dex) for the final solutions.

Following several previous analyses of deep *HST*-based CMDs (e.g., Weisz et al. 2012, 2014b), we masked out the red clump and horizontal branch regions of the observed CMD for the fitting process, as indicated in Figure 5. The physics of these evolutionary phases are highly uncertain (e.g., Gallart

Table 2
Model Parameters

Quantity	Range	Resolution
$(m - M)_0$	20.60–21.10	0.05, 0.01
A_V	0.0–0.5	0.05, 0.01
IMF	Kroupa (2001)	fixed
$\log(\text{age})$	9.0–10.15	0.05
[M/H]	–2.3 to –0.5	0.05
$[\alpha/\text{Fe}]$	–0.2, 0.0, +0.2, +0.4	fixed
Binary fraction	0.1, 0.35, 0.6	fixed

Note. Parameters and their ranges and resolutions used as input into `MATCH`. Parameters with multiple resolutions indicated were solved for iteratively: first through a large search with the coarser resolution and then via a focused search at the higher resolution. α -enhancements are only currently available for the Dartmouth models. We tested several values for the binary fraction, but found that it did not substantially affect determination of the other physical parameters.

et al. 2005), and their inclusion in the CMD fitting process can be problematic. Instead, we rely on the more secure MSTO and subgiant sequences for this analysis.

To model the possible contamination from the MW for stars fainter than where M2FS spectroscopy is available (i.e., $m_{F606W} > 21$), we use a statistical model of the MW foreground based on analysis presented in de Jong et al. (2010).

We determine uncertainties in Crater’s properties differently for the SSP and complex stellar population assumptions. When we require Crater to be an SSP, we compute likelihood values over every possible combination of parameters in the grid. This approach has the advantage of sampling the entirety of likelihood space, which allows for convenient marginalization and full consideration of stochastic effects (e.g., Weisz et al. 2015). Because of the smoothness of the likelihood surface, we marginalize over a finely interpolated grid to measure the most likely values and associated confidence intervals for each parameter to a higher degree of precision than is afforded by the native resolution.

When solving for the full SFH, computing a full grid of solutions is not tractable in a reasonable amount of computational time. Instead, `MATCH` finds the most likely solution and uses an MCMC routine to explore the likelihood surface around it. Specifically, we use a Hamiltonian Monte Carlo (Duane et al. 1987) approach to sampling SFH space as described in Dolphin (2013). For quantifying the uncertainties on Crater’s most likely SFH, we used 5000 MCMC realizations.

5. RESULTS

5.1. Crater as an SSP

As shown in panels (a)–(c) of Figure 5, Crater is well-described by an SSP. Qualitatively, the observed and model CMDs have similar appearances and the MSTO, SGB, and RGB have luminosities, colors, and stellar densities that appear in excellent agreement. This impression is quantitatively reinforced by the residual significance diagram (panel (d)). This diagram shows that the model CMD does an excellent job of reproducing the observed CMDs; there are no systematic mismatches between the model and observed CMDs (e.g., clumps or streaks of all black or white bins), which indicates good data–model agreement.

However, there are two discrepant areas that warrant discussion. First, the luminous blue stars above the predominant MSTO are an area of mismatch. In the event that these are intermediate-age MS stars, our model of an SSP would not be appropriate for Crater, leading to this type of data–model disagreement. On the other hand, these stars may be blue stragglers, which are not included in the PARSEC or Dartmouth libraries, again resulting in a poor data–model match. We discuss the nature of these stars in Section 5.2.

The second poorly fit region is the red clump. As discussed in Section 4, the observed red clump (RC) was masked from the fit. Given its exclusion and outstanding issues in the physics of modeling the red clump (e.g., Gallart et al. 2005), it is not surprising that this feature is not well described by the models. However, because we have excluded it from the fit, it does not affect our characterization of Crater.

The derived physical parameters of Crater are listed in Table 3. In general, the different models produce compatible values for distance, extinction, and total stellar mass. The most notable variations are in age and metallicity. Within the Dartmouth models, the age and metallicity are sensitive to the level of α -enhancement. While the age only exhibits modest variations as a function of $[\alpha/\text{Fe}]$, the mean metallicity varies by ~ 0.6 dex. Of these solutions, the observed CMD is best described by an $[\alpha/\text{Fe}] = +0.4$, although values of 0.0 and +0.2 cannot be ruled out at a confidence level $>95\%$. The model with $[\alpha/\text{Fe}] = -0.2$ provides a drastically worse fit to the CMD. In addition to being a marginally better fit, the model with $[\alpha/\text{Fe}] = +0.4$ also produces a metallicity that is in good agreement with spectroscopic measurements. However, as shown in Figure 6, the color and magnitude differences in isochrones with various amounts of α -enhancements are quite subtle.

To examine the sensitivity of Crater’s parameters to stellar physics, we compare derived parameters for the solar-scaled Dartmouth and PARSEC models (see Figure 6). These two libraries show an age difference of ~ 0.8 Gyr and a metallicity difference of 0.15 dex. The age difference is due to slight variations in the shape of the MSTO and SGB between the two models, as shown in Figure 6. The amplitude of this difference reflects the uncertainties due to choices in underlying stellar physics and is in line with the expected precision for absolute ages of stars and SSPs, which is $\gtrsim 10\%$ of the age of the object (e.g., Soderblom 2010; Cassisi 2014). The ~ 0.15 dex offset metallicity is due to subtle differences in the RGB slopes of the two models.

Finally, we computed the stellar mass and integrated luminosity for Crater by summing up the mass and light from the best-fit SSP models. While this approach does not include the contribution of blue stragglers, it does mitigate the contribution of nonmember stars to the total luminosity. The stellar mass measurements for Crater are listed in Table 3, and the integrated V -band magnitude, from the Dartmouth $[\alpha/\text{Fe}] = +0.4$ model, is listed in Table 1. We calculated uncertainties on these quantities using the SSP solutions that fell within the 68% confidence intervals of the best-fit models. Our total integrated luminosity for Crater is slightly smaller than that presented in Belokurov et al. (2014) and a magnitude larger than that in Laevens et al. (2014). Variations of total luminosity between the stellar models are negligibly small. As an empirical check, we integrated the observed F606W luminosity function, after statistically accounting for likely

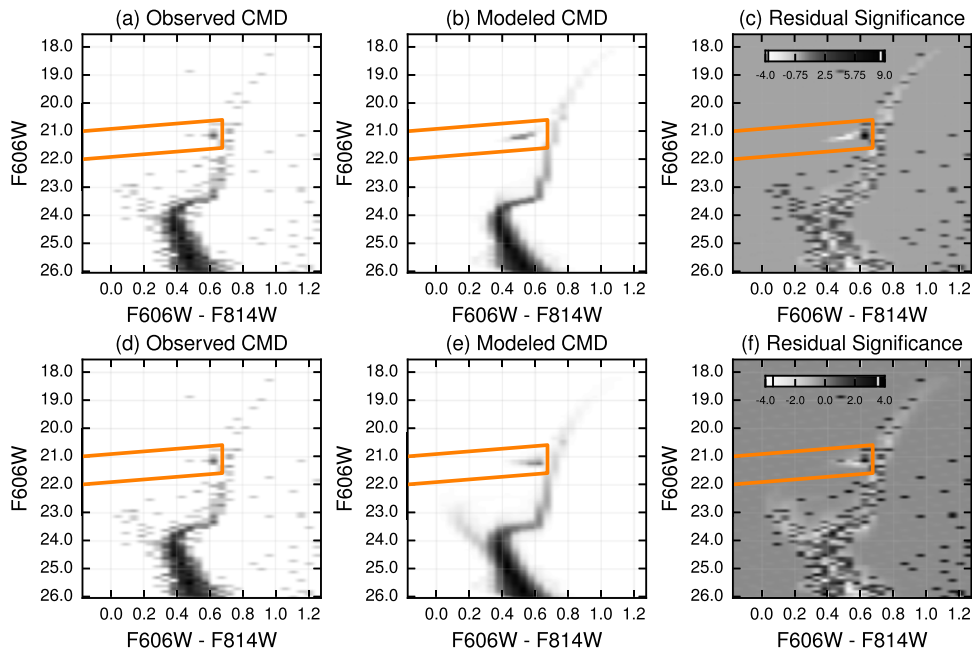


Figure 5. Hess diagrams illustrating the SSP (top row) and full SFH (bottom row) models of the Crater CMD using the Dartmouth models with $[\alpha/\text{Fe}] = +0.4$. The area inside the orange region was excluded from the fitting. The color bars in panels (c) and (f) are in units of σ , where white and black represent the most extreme deviations.

foreground objects, and correcting for distance and extinction, we find $M_{\text{F606W}} \sim -5.35$, which is consistent with the model-based approach described above.

5.2. Crater as a Complex Stellar Population

We now relax the SSP assumption and model the full SFH of Crater, i.e., we allow it to be fit by an arbitrary sum of SSPs as described in Section 4. In panels (d)–(f) of Figure 5, we plot the model CMD for the full SFH fit, and in Figure 7 we show the cumulative SFH (blue; the fraction of stellar mass formed prior to a given epoch) and the best-fitting Dartmouth SSP with $[\alpha/\text{Fe}] = +0.4$ (orange). For simplicity, we only show the results for a single Dartmouth model and note that fitting with other Dartmouth or PARSEC models produces a similar result.

Compared to the SSP scenario, Figure 5 shows that there are fewer highly discrepant regions in the residual significance CMD (panel (f)). This is due to the increased number of free parameters in the model. Blue stars above the MSTO have been modeled by populations of intermediate-age MS stars.

The main result of this analysis is shown in Figure 7. The full SFH shows that $>95\%$ of the stellar mass in Crater formed in a single event around ~ 7.5 Gyr ago. This is fully consistent with the best-fit SSP age as discussed in Section 5.1 and reinforces that Crater is well described by an SSP, even when a complex population is allowed.

The remaining $\sim 5\%$ of the stellar mass formed either slightly before or after the main epoch. The small amount of mass formed prior to ~ 7.5 Gyr ago can be attributed to the code compensating for slight mismatches between the isochrone and observed CMD. Similarly, the small amount of mass formed ~ 3 Gyr ago is the result of fitting the luminous blue stars as MS stars.

However, as illustrated in Figure 8, it is equally plausible that these blue stars are blue stragglers. The left panel shows that single-star isochrones clearly overlap the main locus of blue stars. For comparison, in the right panel, we overplot

select models of blue stragglers, including their evolution off the MS, from Sills et al. (2009). These models are for a slightly more metal-poor population, $[\text{M}/\text{H}] \sim -2.3$, but Sills et al. (2009) suggest that the properties of blue stragglers are not a strong function of metallicity.

Visually, it is not possible to determine whether the single-star or blue straggler model sequences better describe the data. However, there are a few reasons to believe that these stars are blue stragglers. First, the ratio of putative MS to SGB stars is unrealistic for a standard IMF (e.g., Kroupa, Salpeter). If this was a genuine intermediate-age population, we would expect far more MS than SGB stars, given that a star’s SGB phase lasts only $\sim 10\%$ of its MS lifetime. The observed ratio is roughly unity. Second, we have established that Crater is likely a GC, not a dwarf galaxy. Given that all known GCs in the MW host blue stragglers, we expect the same from Crater. Third, a cursory inspection of the spatial distribution of the blue stragglers shows that it is similar to other MW GCs (e.g., Ferraro et al. 2015), although the small number of blue stragglers in Crater precludes anything beyond a qualitative comparison.

6. DISCUSSION

6.1. Dwarf Galaxy or GC?

From our analysis, it is clear that Crater is a GC and not a dwarf galaxy. Its stellar mass is consistent with being formed at a single age and metallicity, within the precision allowed by a given stellar evolution model. The sparse population of blue stars above the main turnoff and SGB can plausibly be explained as blue stragglers and their evolved descendants. Moreover, the complete lack of an ancient population (>10 Gyr) would make Crater unlike any known dwarf galaxy, all of which are known to host ancient, metal-poor populations (e.g., Tolstoy et al. 2009; Brown et al. 2012, 2014; Weisz et al. 2014a). Our finding that Crater is a GC is in line with both

Table 3
Measured Single Stellar Population Properties of Crater

Property	Dartmouth	Dartmouth	Dartmouth	Dartmouth	PARSEC
	$[\alpha/\text{Fe}] = -0.2$	$[\alpha/\text{Fe}] = 0.0$	$[\alpha/\text{Fe}] = +0.2$	$[\alpha/\text{Fe}] = +0.4$	$[\alpha/\text{Fe}] = 0.0$
Age (Gyr)	6.7 ± 0.4	7.5 ± 0.4	7.5 ± 0.4	7.5 ± 0.4	6.7 ± 0.4
$[M/H]$	-1.03 ± 0.02	-1.33 ± 0.03	-1.55 ± 0.04	-1.66 ± 0.04	-1.47 ± 0.03
$(m - M)_0$	20.83 ± 0.03	20.82 ± 0.03	20.82 ± 0.03	20.81 ± 0.03	20.82 ± 0.03
A_V	0.09 ± 0.03	0.10 ± 0.03	0.10 ± 0.03	0.10 ± 0.03	0.11 ± 0.03
Mass ($10^3 M_\odot$)	$9.7^{+0.1}_{-0.05}$	$9.8^{+0.1}_{-0.05}$	$9.8^{+0.1}_{-0.05}$	$9.9^{+0.1}_{-0.05}$	$10.0^{+0.1}_{-0.07}$

Note. Derived properties for Crater as an SSP. We list the most likely value and the 68% confidence intervals. The uncertainties are only statistical in nature, i.e., they scale with the number of stars on the CMD.

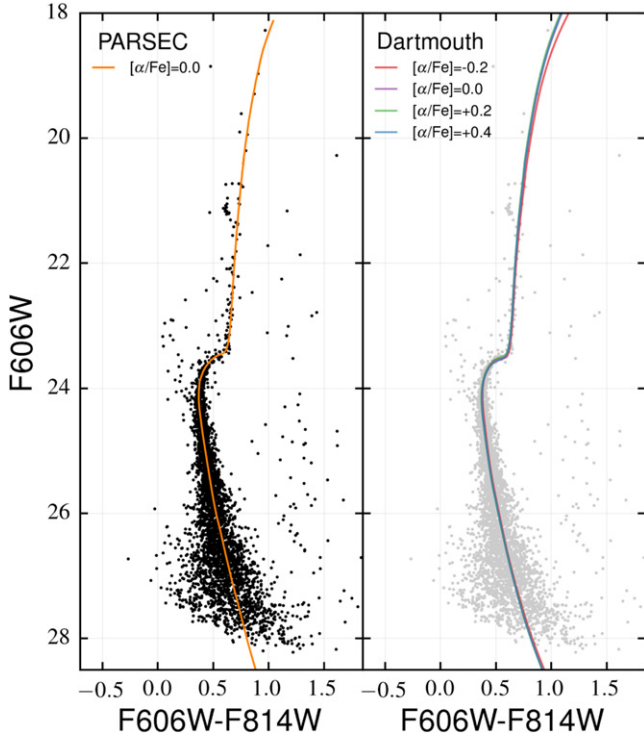


Figure 6. CMDs of Crater with the best-fitting PARSEC and Dartmouth isochrones overplotted. Variations in the inferred physical properties are due to subtle differences in the model shapes of the oldest MSTO, SGB, and slope of the RGB. Points in the right panel have been grayed out to provide increased visual contrast with the isochrones.

Laevens et al. (2014) and Kirby et al. (2015), who reach the same conclusion using different observations. The strongest evidence in favor of Crater being a dwarf is presented by Bonifacio et al. (2015), who find a velocity dispersion in excess of expectations from assuming that Crater is a purely baryonic system. However, this analysis is based on spectroscopy of only two stars with large uncertainties in their velocities. Using larger samples, Kirby et al. (2015) and M. Mateo (2016, in preparation) find velocity dispersions that are consistent with expectations for a stellar system composed entirely of baryons of Crater’s mass. On the whole, the properties of Crater do not satisfy the criteria for being classified as a galaxy as articulated by Willman & Strader (2012).

6.2. An Enigmatic GC

In Figures 9 and 10 we plot Crater’s properties relative to those of the general MW GC population. Data for the MW

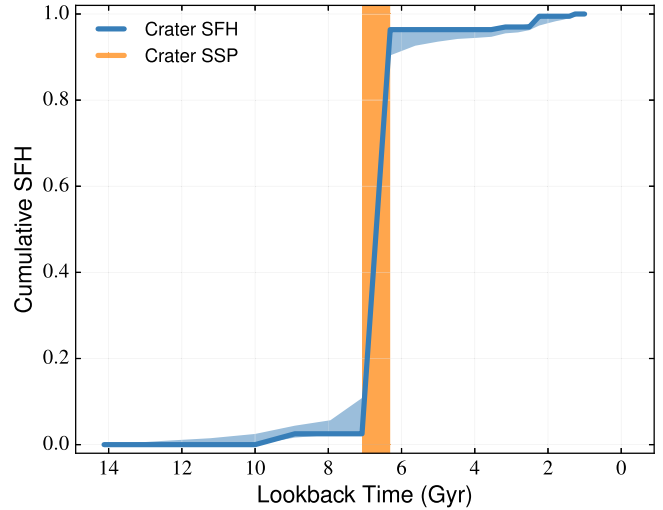


Figure 7. Comparison between the full SFH of Crater (blue) and its best-fit SSP (orange) as measured with the Dartmouth models ($[\alpha/\text{Fe}] = +0.4$). The shaded blue region indicates the 68% confidence interval in the SFH as determined with 5000 MCMC iterations. The full SFH shows that $>95\%$ of Crater’s total stellar mass formed at a single age, which is consistent with it being an SSP. The small percentage of Crater’s stellar mass that formed ~ 3 Gyr ago is due to the code modeling likely blue stragglers as intermediate-age MS stars, and it is unlikely to be genuine intermediate-age star formation.

clusters are drawn from a variety of sources, and owing to the potential for systematics, we only undertake a qualitative comparison of Crater relative to other clusters. Specifically, ages and metallicities of the MW GCs are primarily drawn from Vandenberg et al. (2013), where available, and otherwise from Dotter et al. (2008, 2010). The distances, luminosities, and sizes are taken from the 2010 update to the MW GC catalog of Harris (1996).¹² Properties from the newly discovered halo cluster Kim 2 are from Kim et al. (2015b). We have not included all known MW GCs on this plot. For example, we have excluded some of the lowest-luminosity GCs (e.g., Koposov 1 and 2, Segue 3; Koposov et al. 2007; Belokurov et al. 2010; Fadelly et al. 2011), which do not have well-characterized stellar populations compared to more luminous GCs.

As shown in Figure 9, Crater is among the youngest, largest, and most distant of the MW’s GCs. Although it shares a similar metallicity and distance to several halo GCs (e.g., AM-1, Pal 4), it stands out owing to its young age, which is comparable only to a handful of GCs located within ~ 40 kpc of the Galactic

¹² <http://www.physics.mcmaster.ca/~harris/mwgc.dat>

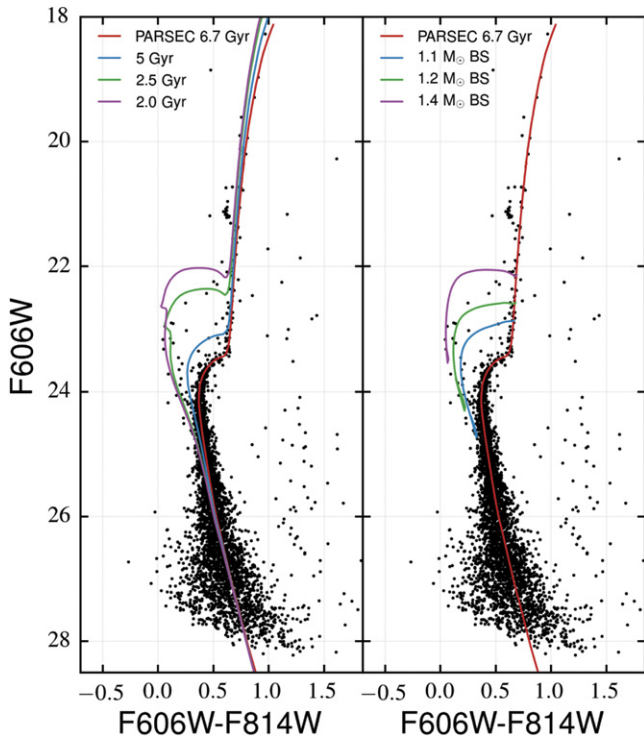


Figure 8. CMDs of Crater with select PARSEC isochones overlaid in the left panel and tracks of collisional blue stragglers from Sills et al. (2009) overlaid on the right. A comparison of the two sets of models illustrates the similarity between the two intermediate-age single stars and blue stragglers.

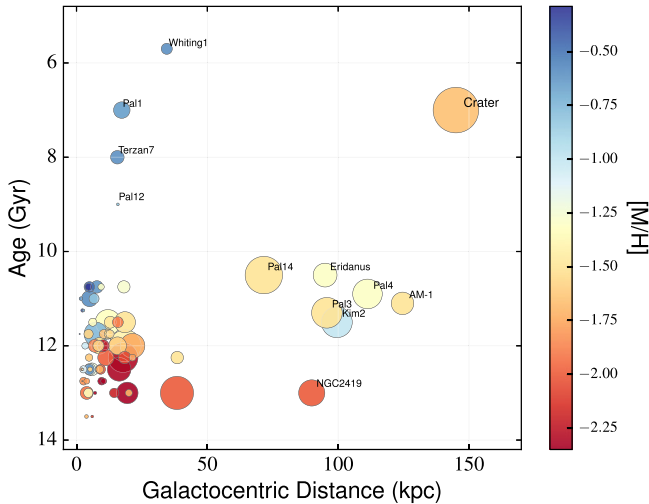


Figure 9. Age, metallicity, half-light radius, and galactocentric distance of Crater relative to the general population of MW GCs. Point sizes are proportional to the cluster half-light radii. Crater is a clear outlier compared to most MW GCs.

center (e.g., Whiting 1, Pal 1, Terzan 7). These young clusters are typically associated with the accretion of Sagittarius; it is clear that Crater is not. Furthermore, Crater exhibits a smaller magnitude difference between the MSTO and horizontal branch (HB) ($\Delta M_V \sim 2.7$) when compared to Galactic center GCs of a similar metallicity ($\Delta M_V \sim 3.0$; e.g., Buonanno et al. 1998).

The unusual properties of Crater provide new insight into how various mechanisms (e.g., major merger, accretion of satellites) contributed to the assembly of the MW. To

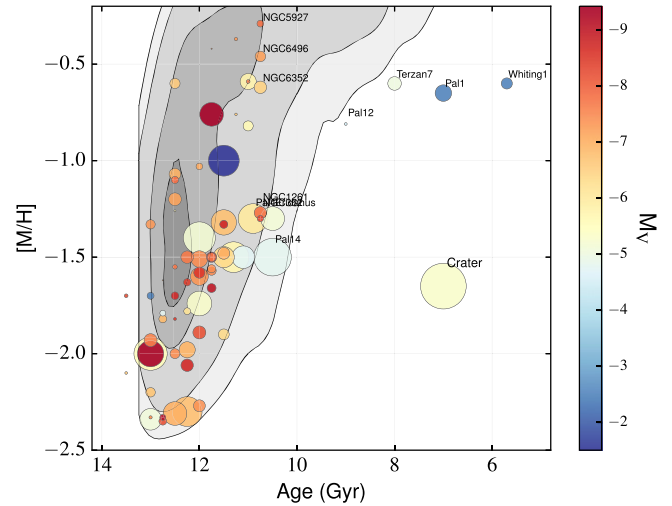


Figure 10. Ages and metallicities of MW GCs, with predictions from the GC formation models of Li & Gnedin (2014) overplotted as contours. The point sizes are proportional to the cluster half-light radii. From darkest to lightest, the contours indicate the expected fraction of GCs: 10%, 50%, 90%, and 97%. The models, which posit that GCs form in major mergers, capture the bulk of the MW cluster populations. However, Crater is a clear outlier, indicating that mechanisms in addition to mergers are necessary to explain the entire MW GC population.

demonstrate this, in Figure 10, we plot the age–metallicity relationship for the population of MW GCs, including Crater, and overplot predictions from the GC formation models presented in Li & Gnedin (2014). These models combine the dark-matter-only Millenium II simulations of Boylan-Kolchin et al. (2009) with a semianalytic model for GC formation as described in Muratov & Gnedin (2010). These models assume that GCs are formed during major mergers, and are in good qualitative agreement with bulk trends for most MW GCs.

However, Crater, along with a handful of other young MW GCs, is a significant outlier compared to the model of Li & Gnedin (2014). This suggests that while major mergers can plausibly explain the bulk of the MW’s GC population, other mechanisms (e.g., accretion of low-mass satellite galaxies) are needed to explain these systems. By virtue of being young, metal-poor, and located in the outer stellar halo, Crater may instead be the signpost of a previously unknown MW accretion event, with its age indicating that such an event occurred more recently than ~ 8 Gyr ago ($z \sim 1$, assuming a Planck cosmology; Planck Collaboration et al. 2014). We discuss the possible origins of Crater further in the following section.

6.3. Where Did Crater Originate?

Given its likely extragalactic origin, we can use the properties of Crater to better understand its host galaxy. Based on its position in the Galaxy, Crater (L_{MS} , B_{MS} , $V_{GSR} = +80.6943$, -5.87460 , $+150 \text{ km s}^{-1}$, where “MS” denotes the Magellanic Stream coordinate system) is well-matched to the location of tidal debris from the Magellanic Stream as predicted by the models of Besla et al. (2012). Furthermore, Crater’s heliocentric velocity of $\sim +150 \text{ km s}^{-1}$ (Kirby et al. 2015) is consistent with the measured gas velocity of the Magellanic Stream of $100\text{--}200 \text{ km s}^{-1}$ (Nidever et al. 2010). Thus, it is plausible that Crater was accreted during an interaction between the MW and the Magellanic Clouds.

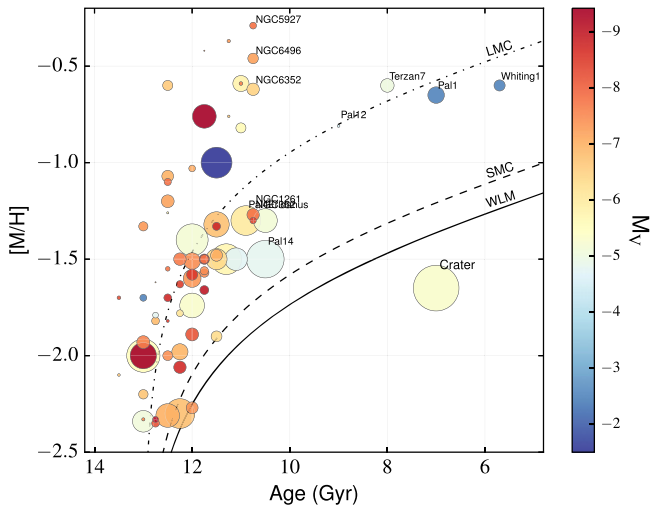


Figure 11. Same as Figure 10, but with the age–metallicity relationships of the LMC, SMC, and WLM as presented in Leaman et al. (2013) overplotted. Assuming that GCs follow their host galaxy’s age–metallicity relationship, we suggest that Crater is likely to have formed in a dwarf galaxy less massive than WLM ($M_{\text{star}}^{z=0} \sim 4 \times 10^7 M_{\odot}$) and possibly in a galaxy similar in mass to Carina or Leo I.

However, as shown in Figure 11, Crater’s age and metallicity are not obviously compatible with the age–metallicity relationships of the LMC or SMC (Leaman et al. 2013). Compared to the SMC age–metallicity relationship, Crater is either too metal-poor for its age or too young for its metallicity. This discrepancy is larger when compared to the LMC.

It may be the case that Crater is simply an anomalous cluster from the SMC. A handful of SMC clusters are known to be offset from the galaxy-wide age–metallicity relationship. A particularly relevant example is that of Lindsay 38, which has an age of ~ 6.5 Gyr and a metallicity of $[M/H] = -1.49$, as determined from deep *HST* imaging presented in Glatt et al. (2008). Its similarity to Crater suggests that it is at least plausible that Crater originated as an anomalous cluster in the SMC before being captured by the MW.

Alternatively, if we assume that clusters should roughly follow their host galaxy’s age–metallicity relationship, it appears that Crater likely originated in a fairly low mass dwarf galaxy. As shown in Figure 11, even relative to a less massive dwarf galaxy, WLM ($M_{\text{star}}^{z=0} \sim 4 \times 10^7 M_{\odot}$; McConnachie 2012), Crater is slightly offset from the age–metallicity relationship. Fornax, which is a factor of ~ 2 less massive than WLM, has a nearly identical age–metallicity relationship. Although both Fornax and WLM contain GCs, they are generally older (> 10 Gyr) and more metal-poor ($[M/H] < -2.0$) than Crater (e.g., Buonanno et al. 1998; Hodge et al. 1999). The exception is Fornax 4, which resembles Crater in metallicity but is 3–4 Gyr older (Buonanno et al. 1999).

Instead, if GCs do trace the age–metallicity relationship of the host, then it is likely that Crater formed in a system similar in mass to Leo I or Carina. Both have had continuous star formation throughout their lifetimes (e.g., Weisz et al. 2014a) and have present-day stellar metallicities similar to Crater. However, the mean metallicity of Carina, as presented in de Boer et al. (2014), does not reach Crater’s value until ~ 5 Gyr ago, indicating that it is not an exact match. Of course, such quantities highly depend on the SFH of a particular

system, and this type of mismatch may suggest that Crater’s progenitor happened to enrich slightly more quickly than Carina. On the other hand, there is no known stream near Crater, which decreases the likelihood of Crater’s accretion being attributable to a dwarf galaxy that was destroyed by the MW.

The authors would like to thank the referee, Michele Bellazzini, for a thorough and helpful report that improved the paper. The authors also thank Cliff Johnson for interesting discussions about blue stragglers, Ryan Leaman for providing dwarf galaxy age–metallicity relationships, Gurtina Besla for her insight into the Magellanic Stream debris, Jieun Choi for detailed comments, Eduardo Balbinot for his discussion on the Magellanic Stream, and Oleg Gnedin and Hui Li for providing results from their GC models. DRW is supported by NASA through Hubble Fellowship grant HST-HF-51331.01 awarded by the Space Telescope Science Institute. M.G.W. is supported by National Science Foundation grants AST-1313045 and AST-1412999. E.O. is supported by NSF grants AST-0807498 and AST-1313006, and M.M. is supported by NSF grants AST-0808043 and AST-1312997. M.G. acknowledges the European Research Council (ERC-StG-335936) and the Royal Society for financial support. Support for this work was provided by NASA through grant number HST-GO-13746.001-A from the Space Telescope Science Institute, which is operated by AURA, Inc., under NASA contract NAS 5-26555. Research leading to these results has also received support from the European Research Council under the European Union’s Seventh Framework Program (FP/2007-2013) ERC Grant Agreement no. 308024. Analysis and plots presented in this paper used IPython and packages from NumPy, SciPy, and Matplotlib (Hunter 2007; Oliphant 2007; Pérez & Granger 2007; Astropy Collaboration et al. 2013).

*Facility:*HST(ACS).

REFERENCES

- Astropy Collaboration, Robitaille, T. P., Tollerud, E. J., et al. 2013, *A&A*, **558**, A33
- Belokurov, V., Irwin, M. J., Koposov, S. E., et al. 2014, *MNRAS*, **441**, 2124
- Belokurov, V., Walker, M. G., Evans, N. W., et al. 2009, *MNRAS*, **397**, 1748
- Belokurov, V., Walker, M. G., Evans, N. W., et al. 2010, *ApJL*, **712**, L103
- Belokurov, V., Zucker, D. B., Evans, N. W., et al. 2006, *ApJL*, **647**, L111
- Belokurov, V., Zucker, D. B., Evans, N. W., et al. 2007, *ApJ*, **654**, 897
- Besla, G., Kallivayalil, N., Hernquist, L., et al. 2012, *MNRAS*, **421**, 2109
- Bonifacio, P., Caffau, E., Zaggia, S., et al. 2015, *A&A*, **579**, L6
- Bovill, M. S., & Ricotti, M. 2009, *ApJ*, **693**, 1859
- Boylan-Kolchin, M., Springel, V., White, S. D. M., Jenkins, A., & Lemson, G. 2009, *MNRAS*, **398**, 1150
- Bressan, A., Marigo, P., Girardi, L., et al. 2012, *MNRAS*, **427**, 127
- Brown, T. M., Tumlinson, J., Geha, M., et al. 2012, *ApJL*, **753**, L21
- Brown, T. M., Tumlinson, J., Geha, M., et al. 2014, *ApJ*, **796**, 91
- Buonanno, R., Corsi, C. E., Castellani, M., et al. 1999, *AJ*, **118**, 1671
- Buonanno, R., Corsi, C. E., Zinn, R., et al. 1998, *ApJL*, **501**, L33
- Cassisi, S. 2014, in *EAS Publications Ser. 65, The Age of Stars*, ed. Y. Lebreton, D. Valls-Gabaud, & C. Charbonnel (Paris: EDP Science), 17
- de Boer, T. J. L., Tolstoy, E., Lemasle, B., et al. 2014, *A&A*, **572**, A10
- de Jong, J. T. A., Yanny, B., Rix, H.-W., et al. 2010, *ApJ*, **714**, 663
- Dolphin, A. E. 2000, *PASP*, **112**, 1383
- Dolphin, A. E. 2002, *MNRAS*, **332**, 91
- Dolphin, A. E. 2013, *ApJ*, **775**, 76
- Dotter, A., Chaboyer, B., Jevremović, D., et al. 2008, *ApJS*, **178**, 89
- Dotter, A., Sarajedini, A., Anderson, J., et al. 2010, *ApJ*, **708**, 698
- Duane, S., Kennedy, A. D., Pendleton, B. J., & Roweth, D. 1987, *PhLB*, **195**, 216
- Fadely, R., Willman, B., Geha, M., et al. 2011, *AJ*, **142**, 88

- Ferraro, F. R., Lanzoni, B., Dalessandro, E., Mucciarelli, A., & Lovisi, L. 2015, Blue Straggler Stars in Globular Clusters: A Powerful Tool to Probe the Internal Dynamical Evolution of Stellar Systems, ed. H. M. J. Boffin, G. Carraro, & G. Beccari (Berlin: Springer), 99
- Ford, H. C., Bartko, F., Bely, P. Y., et al. 1998, Proc. SPIE, 3356, 234
- Gallart, C., Zoccali, M., & Aparicio, A. 2005, ARA&A, 43, 387
- Gieles, M., & Zocchi, A. 2015, MNRAS, 454, 576
- Girardi, L., Groenewegen, M. A. T., Hatziminaoglou, E., & da Costa, L. 2005, A&A, 436, 895
- Glatt, K., Grebel, E. K., Sabbi, E., et al. 2008, AJ, 136, 1703
- Harris, W. E. 1996, AJ, 112, 1487
- Hodge, P. W., Dolphin, A. E., Smith, T. R., & Mateo, M. 1999, ApJ, 521, 577
- Hunter, J. D. 2007, CSE, 9
- Irwin, M. J., Belokurov, V., Evans, N. W., et al. 2007, ApJL, 656, L13
- Kim, D., Jerjen, H., Mackey, D., Da Costa, G. S., & Milone, A. P. 2015a, ApJL, 804, L44
- Kim, D., Jerjen, H., Milone, A. P., Mackey, D., & Da Costa, G. S. 2015b, ApJ, 803, 63
- King, I. R. 1966, AJ, 71, 64
- Kirby, E. N., Simon, J. D., & Cohen, J. G. 2015, ApJ, 810, 56
- Koposov, S., de Jong, J. T. A., Belokurov, V., et al. 2007, ApJ, 669, 337
- Koposov, S. E., Belokurov, V., Torrealba, G., & Wyn Evans, N. 2015a, ApJ, 805, 130
- Koposov, S. E., Casey, A. R., Belokurov, V., et al. 2015b, ApJ, 811, 62
- Kroupa, P. 2001, MNRAS, 322, 231
- Laevens, B. P. M., Martin, N. F., Bernard, E. J., et al. 2015a, ApJL, 813, L44
- Laevens, B. P. M., Martin, N. F., Ibata, R. A., et al. 2015b, ApJL, 802, L18
- Laevens, B. P. M., Martin, N. F., Sesar, B., et al. 2014, ApJL, 786, L3
- Leaman, R., Venn, K. A., Brooks, A. M., et al. 2013, ApJ, 767, 131
- Li, H., & Gnedin, O. Y. 2014, ApJ, 796, 10
- Mackey, A. D., & Gilmore, G. F. 2004, MNRAS, 355, 504
- Martin, N. F., Nidever, D. L., Besla, G., et al. 2015, ApJL, 804, L5
- Mateo, M., Bailey, J. I., Crane, J., et al. 2012, Proc. SPIE, 8446, 4
- McConnachie, A. W. 2012, AJ, 144, 4
- Muratov, A. L., & Gnedin, O. Y. 2010, ApJ, 718, 1266
- Nidever, D. L., Majewski, S. R., Butler Burton, W., & Nigra, L. 2010, ApJ, 723, 1618
- Oliphant, T. E. 2007, CSE, 9
- Pérez, F., & Granger, B. E. 2007, CSE, 9
- Planck Collaboration, Ade, P. A. R., Aghanim, N., et al. 2014, A&A, 566, A54
- Sills, A., Karakas, A., & Lattanzio, J. 2009, ApJ, 692, 1411
- Simon, J. D., Drlica-Wagner, A., Li, T. S., et al. 2015, ApJ, 808, 95
- Simon, J. D., & Geha, M. 2007, ApJ, 670, 313
- Soderblom, D. R. 2010, ARA&A, 48, 581
- The DES Collaboration, Bechtol, K., Drlica-Wagner, A., et al. 2015a, ApJ, 807, 50
- The DES Collaboration, Drlica-Wagner, A., Bechtol, K., et al. 2015b, ApJ, 813, 109
- Tolstoy, E., Hill, V., & Tosi, M. 2009, ARA&A, 47, 371
- VandenBerg, D. A., Brogaard, K., Leaman, R., & Casagrande, L. 2013, ApJ, 775, 134
- Walker, M. G., Mateo, M., Olszewski, E. W., et al. 2015, ApJ, 808, 108
- Weisz, D. R., Dalcanton, J. J., Williams, B. F., et al. 2011, ApJ, 739, 5
- Weisz, D. R., Dolphin, A. E., Skillman, E. D., et al. 2014a, ApJ, 789, 147
- Weisz, D. R., Johnson, L. C., Foreman-Mackey, D., et al. 2015, ApJ, 806, 198
- Weisz, D. R., Skillman, E. D., Hidalgo, S. L., et al. 2014b, ApJ, 789, 24
- Weisz, D. R., Zucker, D. B., Dolphin, A. E., et al. 2012, ApJ, 748, 88
- Williams, B. F., Lang, D., Dalcanton, J. J., et al. 2014, ApJS, 215, 9
- Willman, B., Blanton, M. R., West, A. A., et al. 2005a, AJ, 129, 2692
- Willman, B., Dalcanton, J. J., Martinez-Delgado, D., et al. 2005b, ApJL, 626, L85
- Willman, B., & Strader, J. 2012, AJ, 144, 76
- York, D. G., Adelman, J., Anderson, J. E., Jr., et al. 2000, AJ, 120, 1579
- Zucker, D. B., Belokurov, V., Evans, N. W., et al. 2006a, ApJL, 643, L103
- Zucker, D. B., Belokurov, V., Evans, N. W., et al. 2006b, ApJL, 650, L41